ISSN 1066-3622, Radiochemistry, 2018, Vol. 60, No. 3, pp. 316–322. © Pleiades Publishing, Inc., 2018.
Original Russian Text © S.V. Yudintsev, 2018, published in Radiokhimiya, 2018, Vol. 60, No. 3, pp. 273–278.

Behavior of Host Materials with Surrogates of the Rare Earth–Actinide Fraction under Ion Irradiation

S. V. Yudintsev*[a,b]

[a] *Institute of Geology of Ore Deposits, Petrography, Mineralogy, and Geochemistry, Russian Academy of Sciences, Staromonetnyi per. 35, Moscow, 119071 Russia*
[b] *Frumkin Institute of Physical Chemistry and Electrochemistry, Russian Academy of Sciences, Leninskii pr. 31, korp. 4, Moscow, 119071 Russia*
**e-mail: syud@igem.ru*

Received July 12, 2017

Abstract—The behavior of rare earth titanate phases of monoclinic and orthorhombic symmetry under ion irradiation was studied. Three samples contain a set of rare earth elements (REE), and in one sample the high-level waste (HLW) is simulated by neodymium. The samples were prepared by sintering at 1400°C or cold crucible induction melting followed by melt crystallization. The samples were irradiated with 1-MeV Kr^{2+} ions at temperatures in the range 298–1023 K on a tandem installation consisting of an ion accelerator and a transmission electron microscope. The critical amorphization doses for the samples at 298 K were (1.5–2.5) × 10^{14} ion cm^{-2}. These values correspond to those for monoclinic titanates $Nd_2Ti_2O_7$ and $La_2Ti_2O_7$, are close to those for REE–Ti pyrochlores and brannerite, and are lower by an order of magnitude than those for zirconolites at the same irradiation mode. The critical amorphization temperature of the phases studied (900 K) is comparable to that of $Nd_2Ti_2O_7$ (920 K), but higher than that of $La_2Ti_2O_7$ (840 K). Close radiation resistance of the $REE_2Ti_2O_7$ and $REE_4Ti_9O_{24}$ phases in which the rare earth elements are represented by a mixture of elements similar in composition to their set in spent nuclear fuel and liquid HLW from its reprocessing or solely by Nd confirms the assumption that Nd is a suitable surrogate for the whole rare earth–actinide fraction.

Keywords: rare earth–actinide fraction, immobilization, monoclinic rare earth titanate, orthorhombic rare earth titanate, ion irradiation, radiation resistance, borehole repository

DOI: 10.1134/S1066362218030153

Disposal of nuclear power engineering waste containing long-lived radionuclides in boreholes of up to 5 km depth is a promising way of the waste management [1, 2]. Waters in such zones are isolated from the surface for millions of years; therefore, the waste repository will not pose hazard to humans. This approach is particularly topical for high-level waste (HLW) containing actinides. Processes for recovering rare earth elements (REE) and transplutonium actinides from HLW from spent nuclear fuel (SNF) regeneration have been developed [3]; one of them is implemented at the Mayak Production Association [4]. The major components of this fraction are cerium-group REE (Nd, La, Ce, Sm, Pr); the relative content of actinides (Am, Cm) does not exceed 5 wt %. Various REE phases are considered as host materials for isolation of this fraction [5], namely, phosphates (the natural analog is monazite), silicates (britholite), zirconates, and titanates (pyrochlore, perovskite, brannerite). Rare earth titanates of the compositions $REE_2Ti_2O_7$ (space group $P2_1$, $Z = 4$) and $REE_4Ti_9O_{24}$ (*Fddd*, $Z = 16$) have been suggested for this purpose [6, 7]. Interest in these phases is due to high content of simulated waste (48–67 wt %) and very low solubility in heated aqueous solutions and brines [8, 9].

Another important characteristic of a crystalline host material is its behavior upon decay of actinide nuclides [10–13]. The collision of α-particles (He ions) and heavy recoil nuclei with atoms causes their displacement from the initial positions in the structure of the host material and finally in its disordering (amorphization). As a result, the stability of the host material in the solution decreases, and the radionuclide release rate increases. The α-decay in host materials can be efficiently simulated by ion irradiation. This approach is used for more than 30 years for rapid evaluation of the radiation resistance of materials [14, 15]. Its advantages are quick acquisition of large irradiation doses, observation of the radiation damage in situ, i.e., di-

rectly in the course of irradiation using a transmission electron microscope, possibility of varying the temperature in the course of irradiation from 15 to 1300 K, and absence of induced activity in the samples. As a result, the quantitative characteristics of the radiation resistance are determined: critical dose (D_c) at room temperature or 0 K and critical amorphization temperature (T_c). D_c is the irradiation dose at which a crystalline host material becomes X-ray and electron beam amorphous. On heating, the atoms return to their initial structural positions. Therefore, the critical dose increases with temperature. Above the critical temperature (T_c), the material does not undergo amorphization at any irradiation doses.

Irradiation is usually performed using ions of inert gases (He, Ne, Ar, Kr, Xe) with the energy of 0.7–2.0 MeV [15]. They penetrate into the substance to a depth depending on the ion energy and mass. For 1-MeV Kr^+ ions, the penetration depth is about 400 nm [16], which requires special methods for studying the irradiated material, e.g., small-angle X-ray diffraction. Ions of higher energy in the range from 100 MeV to 3 GeV, e.g., Xe (167 MeV), Ta (2 GeV), or Au (2.2 GeV), came into use for this purpose only recently [17–19]. These ions penetrate into the material to a depth of 20–100 μm, and at a half of their range the energy loss of the ions due to their collision with atoms occurs at a constant rate, 20–50 keV nm^{-1}. As a result, the structural disturbances in a large volume of the target are uniform, which allows studying the substance amorphization using such methods as synchrotron X-ray diffraction, X-ray absorption spectroscopy, and Raman spectroscopy [17] along with traditional methods of transmission electron microscopy

Numerous original papers and reviews deal with the behavior of solid target materials upon irradiation. The amorphization doses determined by ion irradiation, incorporation of short-lived actinides, and analysis of related natural radioactive minerals were found to coincide [11]. The radiation resistance of phases of similar structure depends on their composition. In REE phases of pyrochlore structure, the critical doses and amorphization temperatures depend on particular rare earth element [11, 13, 15, 19–21]. In irradiation of pyrochlores $REE_2Ti_2O_7$ (298 K, 1 MeV Kr^+), D_c increases by a factor of 4 in going from terbium to lutetium pyrochlore, whereas T_c decreases from 1120 to 480 K [20, 21] with a decrease in the ionic radius from 1.08 (Sm^{3+}) to 0.98 Å (Lu^{3+}). The higher is D_c and the lower is T_c, the more resistant is the given phase to irradiation. Thus, $Lu_2Ti_2O_7$ exhibits the highest stability among all the REE–titanate pyrochlores.

Monoclinic REE titanates were studied only in several works. The stability of $La_2Ti_2O_7$ and $Nd_2Ti_2O_7$ under irradiation with ions of both relatively low (1 MeV Kr) and high (2 GeV Ta) energies was studied [17, 22, 23]. These results will be considered in the next sections of the paper. The radiation resistance of orthorhombic $REE_4Ti_9O_{24}$ phases was not studied previously. For more reliable evaluation of the radiation resistance of the host materials, the sample composition should be close to the real HLW composition. In the case of REE–actinide fraction of the waste, this means that the sample should contain not a single element (La or Nd) but the whole set of elements present in this fraction.

We have studied the behavior of four samples of monoclinic and orthorhombic REE titanates under irradiation with 1-MeV Kr^{2+} ions. Three samples (T18, T20, Imcc-2) contained a multicomponent mixture of rare earth elements, and in one sample (Imcc-9) the HLW is simulated by Nd. The samples were prepared by sintering at 1400°C (T18, T20) or by cold crucible induction melting (Imcc-2, Imcc-9). They were examined by X-ray diffraction analysis and by scanning and transmission electron microscopy [6, 7], including examination with a high-resolution device (Fig. 1). Irradiation with 1-MeV Kr^{2+} ions (Fig. 2) was performed in the temperature range 298–1023 K in the Argonne National Laboratory (the United States) on an installation consisting of an ion accelerator and a Hitachi H-9000NAR transmission electron microscope.

Prior to discussing the data on the radiation resistance of monoclinic and orthorhombic REE titanates, let us consider their crystal-chemical features and the composition of the irradiated samples.

CRYSTAL-CHEMICAL FEATURES OF MONOCLINIC AND ORTHORHOMBIC REE TITANATES

The $REE_2Ti_2O_7$ phases crystallize in one of two structural types: cubic pyrochlore (space group $Fd\bar{3}m$) or monoclinic perovskite ($P2_1$) type. The first type is characteristic of heavy and middle rare earth elements with small ionic radius (Y, Yb–Sm). Large REE^{3+} ions (Nd, Ce, La) form the perovskite phase. This is a particular case of monoclinic series of compounds $A_nB_nO_{3n+2}$ ($1 < n < \infty$), where $n = 4$. This structure is characteristic of REE titanates and of alkaline earth

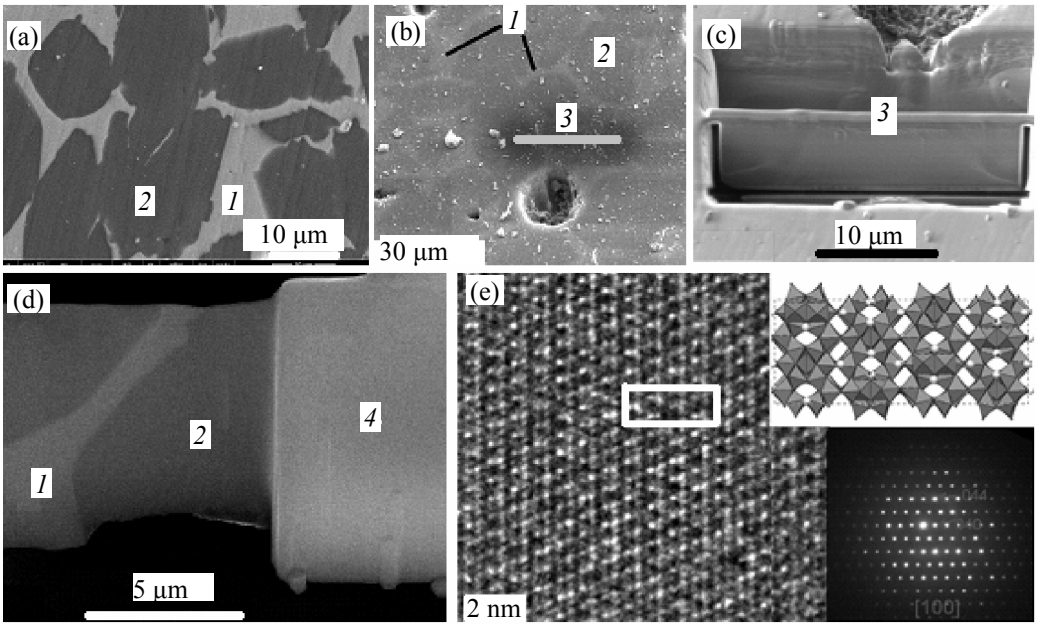

Fig. 1. (a–d) SEM and (e) TEM images of sample Imcc-2 taken as example. (*1*) Rhombic titanate $REE_4Ti_9O_{24}$, (*2*) rutile TiO_2, (*3*) part of the section taken for TEM examination, and (*4*) sample holder. Figure 1e shows the electron diffraction pattern and image of the $REE_4Ti_9O_{24}$ structure, taken with a high-resolution electron microscope; the rectangle bounds the structural fragment corresponding to the unit cell.

niobates and tantalates, e.g., $Ca_2Nb_2O_7$ [24]. Under common conditions (298 K, 1 atm), the structure of pyrochlore type (Fig. 3a) is characteristic of phases of the composition $A_2B_2O_7$, in which the ratio of the ionic radii (r_A/r_B) varies from 1.46 to 1.78. At the ratios lower than 1.46, a fluorite-type structure ($Fm\bar{3}m$) is stable, whereas at ratios higher than 1.78 (with La or Nd occupying position A, and Ti, position B), the monoclinic structure ($P2_1$) with perovskite-type layers is formed (Fig. 3b). In this structure, layers of TiO_6 octahedra sharing common vertices alternate with layers of REE atoms. The REE cations (La) form four different polyhedra and are surrounded by seven to nine oxygen atoms, and the Ti cations have an octahedral surrounding [17]. In the structure of orthorhombic $REE_4Ti_9O_{24}$ (space group *Fddd*) [25], TiO_6 octahedra

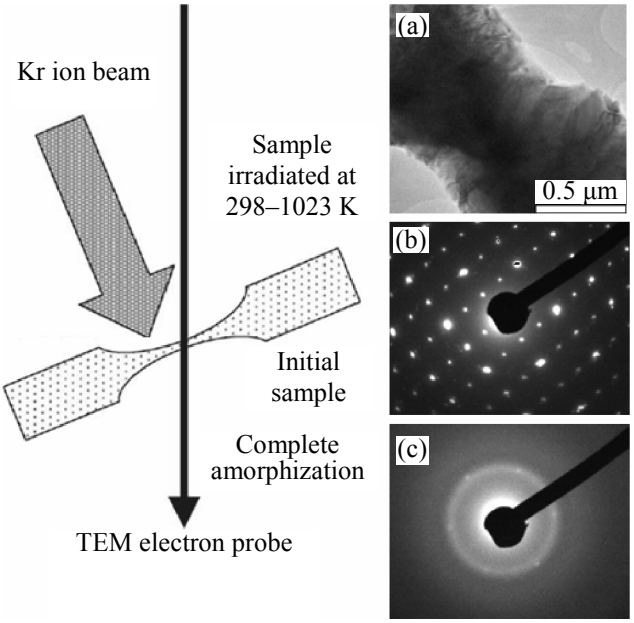

Fig. 2. Scheme of the experiment on irradiation of a grain of monoclinic REE titanate with 1-MeV Kr^{2+} ions: (a) initial sample particle, (b) electron diffraction pattern before irradiation, and (c) structure amorphization observed after irradiation at 298 K to a dose of 2.5×10^{14} ion cm^{-2}.

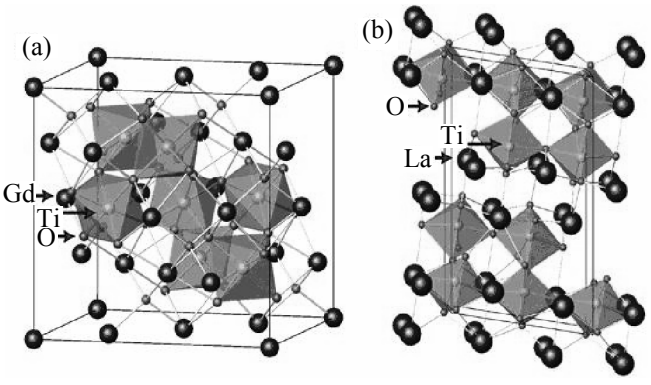

Fig. 3. Unit cells of (a) $Gd_2Ti_2O_7$ (space group $Fd\bar{3}m$) and (b) $La_2Ti_2O_7$ ($P2_1$) phases.

Compositions of major phases[a] in samples taken for irradiation experiments (wt %, SEM/EDX data)

Sample	TiO_2	ZrO_2	La_2O_3	Ce_2O_3	Pr_2O_3	Nd_2O_3	Sm_2O_3	Eu_2O_3	Gd_2O_3	Y_2O_3
T18 (mt)	33.1	0.7	10.4	17.0	6.4	23.6	4.2	1.1	1.3	2.2
T20 (mt)	33.4	–	8.9	16.0	6.0	25.1	5.2	1.4	1.2	2.9
Imcc-2 (rt)	50.4	3.0	5.0	10.9	3.5	19.8	3.1	1.2	1.2	1.9
Imcc-9 (rt)	51.2	1.0	–	–	–	47.8	–	–	–	–

[a] Phase formulas: T18 (mt), $(La_{0.31}Ce_{0.50}Pr_{0.19}Nd_{0.67}Sm_{0.12}Eu_{0.03}Gd_{0.03}Y_{0.09})(Zr_{0.03}Ti_{1.97})O_{6.89}$; T20 (mt), $(La_{0.26}Ce_{0.47}Pr_{0.17}Nd_{0.71}Sm_{0.14}Eu_{0.04}Gd_{0.03}Y_{0.12})Ti_{2.0}O_{6.92}$; Imcc-2 (rt), $(La_{0.43}Ce_{0.92}Pr_{0.30}Nd_{1.63}Sm_{0.25}Eu_{0.10}Gd_{0.09}Y_{0.23})(Ti_{8.71}Zr_{0.34})O_{24.01}$; Imcc-9 (rt), $Nd_{3.96}(Ti_{8.92}Zr_{0.12})O_{23.94}$. (mt) Monoclinic titanate and (rt) rhombic titanate; dash: component not introduced.

share common vertices and edges to form a three-dimensional framework. Two of three REE atoms are surrounded by six O atoms, and the third REE atom, by eight O atoms. The structural unit of the crystal lattice is a cluster of 16 TiO_6 octahedra (Fig. 4), with the REE atoms located in the framework channels oriented along (110).

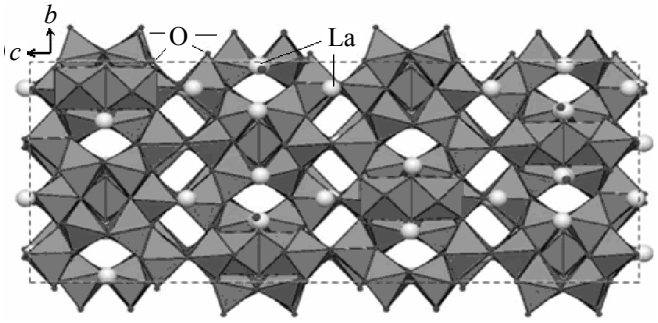

Fig. 4. Structure of the $La_4Ti_9O_{24}$ phase (space group *Fddd*), view along (100).

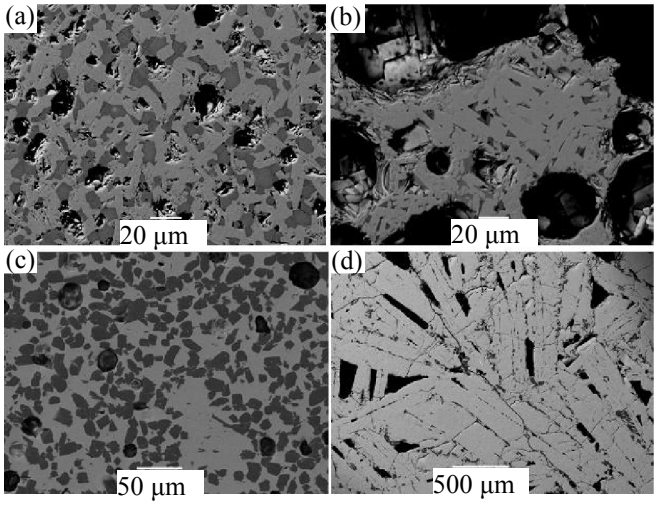

Fig. 5. SEM–EDX images of samples (a) T18, (b) T20, (c) Imcc-2, and (d) Imcc-9. Light areas: (a, b) monoclinic REE titanate and (c, d) orthorhombic REE titanate. Dark areas: (a, b) pyrochlore and (c, d) rutile.

REE TITANATE SAMPLES FOR STUDYING RADIATION RESISTANCE

We took for irradiation two samples with monoclinic titanate $REE_2Ti_2O_7$ of multicomponent composition (T18, T20) and two samples with orthorhombic titanate $REE_4Ti_9O_{24}$, one of which was also multicomponent (Imcc-2) and the other (Imcc-9) contained only Nd as a surrogate of actinide waste. The samples also contained (Fig. 5) 5 to 20% pyrochlore (T18, T20) or 10–50% rutile (Imcc-2, Imcc-9). The compositions of the phases are given in the table, and their formulas are calculated assuming the sum of atomic amounts of Ti + Zr equal to 2 (monoclinic titanate) or the sum of the cations equal to 13 (orthorhombic titanate). According to X-ray diffraction data, the characteristics of these phases are similar to those of the reference compounds $Nd_2Ti_2O_7$ (no. 33-0942) and $Nd_4Ti_9O_{24}$ (no. 81-0950) from the PDFWIN-2 international database [26].

The samples were prepared by irradiation with 1-MeV Kr^{2+} ions at temperatures in the range 298–1023 K and ion flux density of 10^{12} ion cm^{-2} s^{-1}. This procedure simulates most adequately the effect exerted on the crystal structure by recoil nuclei arising in α-decay of actinides [11]. We performed eight irradiation runs. The structural changes were monitored in the course of irradiation (in situ) with a transmission electron microscope. With increasing irradiation dose, the reflection intensities decrease (Figs. 6a–6d), and broad rings appear in the electron diffraction pattern. This is caused by gradual disordering of atoms in the structure of the substance and by its amorphization.

At 298 K, weak reflections remain at the maximal irradiation dose of 2.5×10^{14} ion cm^{-2}. As the temperature is increased over 700 K, the amorphization doses appreciably increase (Figs. 6e–6h). The data obtained for monoclinic and orthorhombic REE titanates of multicomponent (T18, T20, Imcc-2) or simple

(Imcc-9) composition fall on a common curve (Fig. 7), allowing T_c for these phases to be estimated at 900 K. In the general form, the temperature dependence of D_c is described by the formula [27] $D_c = D_0/\{1 - \exp[(E_a/k)(T_c^{-1} - T^{-1})]\}$, where D_c is the critical amorphization dose at the measurement temperature T; T_c, critical temperature; D_0, critical dose at $T = 0$ K; E_a, activation energy of healing of radiation defects in the structure; and k, Boltzmann constant.

The critical doses at 298 K for the samples that we studied are (1.5–2.5) × 10^{14} ion cm^{-2}. These values correspond to those for monoclinic titanates $Nd_2Ti_2O_7$ and $La_2Ti_2O_7$ (1.9 × 10^{14} and 2.2 × 10^{14} ion cm^{-2} [22, 23]), are close to those for REE–Ti-pyrochlores [20] and brannerite [28], but are lower by an order of magnitude than those for zirconolites at the same irradiation mode [29]. The critical temperature of the phases that we studied is estimated at 900 K, which is close to the value for $Nd_2Ti_2O_7$ (920 K) but is somewhat higher than the value of 840 K determined for $La_2Ti_2O_7$ [22, 23].

DISCUSSION

To characterize the damage of the crystalline structure caused by different kinds of irradiation, the irradiation doses are converted into universal quantities, displacements per atom (dpa). A special computer program, SRIM-2000, is used for this purpose [30]. In irradiation with 1-MeV Kr^{2+} ions, the fluence of 10^{14} ion cm^{-2} approximately corresponds to 0.1 dpa. For example, for REE titanate pyrochlores [16], the following critical doses were obtained (ion cm^{-2}; in parentheses, dpa): $Sm_2Ti_2O_7$ 2.18 × 10^{14} (0.26), $Eu_2Ti_2O_7$ 1.97 × 10^{14} (0.23), $Gd_2Ti_2O_7$ 2.57 × 10^{14} (0.29), $Dy_2Ti_2O_7$ 2.0 × 10^{14} (0.25), and $Er_2Ti_2O_7$ 2.22 × 10^{14} (0.25). Such correlation was revealed in ion irradiation of titanates of murataite structure, ferrites of garnet structure, and other host materials [31–33].

The behavior of titanate pyrochlores under irradiation was studied in most detail in connection with their possible use as host materials for plutonium, REE–actinide, and actinide fractions [21, 32]. The critical doses that we obtained for orthorhombic and monoclinic titanates at 298 K are estimated at 0.2–0.3 dpa, which is close to the data obtained for the majority of actinide host materials [11–13, 31]. Large differences are observed only in the critical amorphization temperature. In particular, for REE titanate pyrochlores it varies from 480 K for $Lu_2Ti_2O_7$ to 1120 [20] and even 1240 K for $Gd_2Ti_2O_7$ [22]. An important role of this parameter is that, if the temperature in the repository will be higher than T_c, the host material will not undergo amorphization at any irradiation dose and will remain in the crystalline state. We have estimated [34] the possible temperature around a cylindrical container with the host material of the REE–actinide fraction in relation to its size (block diameter), waste content, and storage time before final disposal in the borehole. As a result, we obtained the curves describing a decrease in the temperature with time in the center and on the surface of the host material after loading into the repository. The time dependence of the temperature for one of such scenarios (block diameter 20 cm, waste content of the host material 40 wt %, preliminary storage for 10 years) reaches a maximum of 573 K in 5 years after the waste disposal and decreases to 393 K in 100 years. It is necessary to add to these values the geothermal gradient, which can

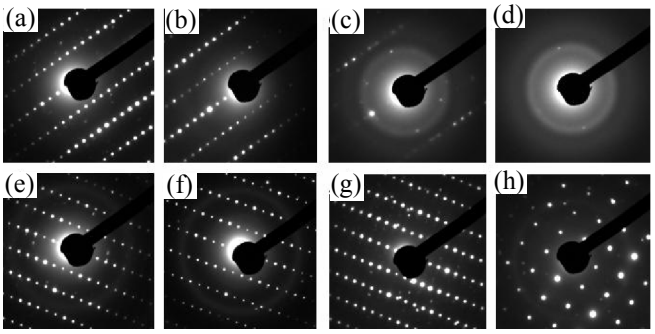

Fig. 6. Evolution of electron diffraction patterns of monoclinic titanate in T18 sample in the course of irradiation at (a–d) 298 and (e–h) 1023 K to different fluences (ion cm^{-2}): (a, e) before irradiation, (b, f) 1.25 × 10^{14}, (c) 1.88 × 10^{14}, (d) 2.5 × 10^{14}, (g) 5.0 × 10^{14}, and (h) 15.0 × 10^{14}.

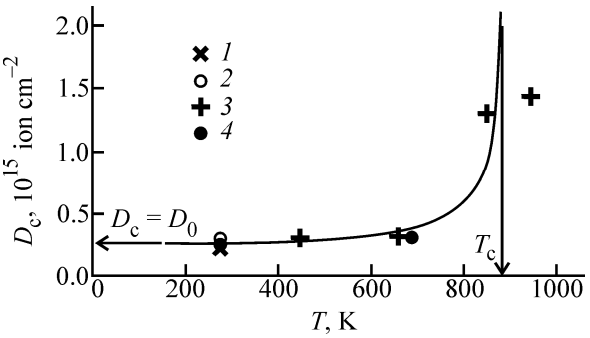

Fig. 7. Temperature dependence of the critical dose of irradiation of REE titanates with 1-MeV Kr^{2+} ions: (*1*) T18, (*2*) T20, (*3*) Imcc-2, and (*4*) Imcc-9.

reach 100–150 K at depths of 3–5 km. That is, the actinide host material will occur in a deep borehole repository for many decades at temperatures of the order of 600 K. Although this value is lower than the critical temperature of REE titanates, estimated at 900 K, such conditions can significantly decelerate the disordering of the host material structure under the action of the actinide decay. As found previously [17], the samples of $Gd_2Ti_2O_7$ ($Fd\bar{3}m$) and $La_2Ti_2O_7$ ($P2_1$), amorphized by irradiation with 2-GeV Ta ions, behaved differently: the titanate of pyrochlore structure ($Gd_2Ti_2O_7$) restored the initial structure at 1123 K, whereas for monoclinic titanate ($La_2Ti_2O_7$) this occurred at 1048 K, i.e., at a temperature lower by 75 K. Healing of radiation defects in $La_2Ti_2O_7$ starts at 943 K, and in the $Gd_2Ti_2O_7$ phase, only at 1063 K. The temperature fields in a borehole repository and their effect on amorphization of crystalline host materials require additional analysis.

It should be noted in conclusion that the $REE_2Ti_2O_7$ and $REE_4Ti_9O_{24}$ phases, where rare earth elements are represented by a mixture of elements similar to that present in spent nuclear fuel and HLW from its reprocessing and solely by Nd, exhibit similar resistance to the ion irradiation. This fact confirms our assumption [6, 7] that Nd is the most suitable surrogate for the REE–actinide HLW fraction.

ACKNOWLEDGMENTS

The study was financially supported by the Russian Foundation for Basic Research (project no. 17-05-00030). The author is grateful to M.Yu. Kalenova and S.V. Stefanovsky for placing titanate samples in his disposal and to B.S. Nikonov and M.S. Nikol'skii for assisting in their study. The ion irradiation was performed by Weixing Li (Stanford University, the United States).

REFERENCES

1. Ringwood, A.E., *Mineral. Mag*., 1985, vol. 49, pp. 159–176.
2. Gibb, F.G.F., Travis, K.P., and Hesketh, K.W., *Miner. Mag*., 2012, vol. 76, pp. 3003–3017.
3. Kopyrin, A.A., Karelin, A.I., and Karelin, V.A., *Tekhnologiya proizvodstva i radiokhimicheskoi pererabotki yadernogo topliva* (Technology of Production and Radiochemical Reprocessing of Nuclear Fuel), Moscow: Atomenergoizdat, 2006. 576 c.
4. Logunov, M.V., Tananaev, I.G., and Myasoedov, B.F., in *Trudy konferentsii "Fundamental'nye aspekty bezopasnogo zakhoroneniya RAO v geologicheskikh formatsiyakh"* (Proc. Conf. "Fundamental Aspects of Safe Disposal of Radioactive Waste in Geological Formations"), Moscow: Granitsa, 2013, pp. 94–96.
5. Stefanovsky, S.V. and Yudintsev, S.V., *Russ. Chem. Rev.*, 2016, vol. 85, no. 9, pp. 962–994.
6. Yudintsev, S.V., Stefanovsky, S.V., Nikonov, B.S., et al., *Radiochemistry*, 2015, vol. 57, no. 2, pp. 187–199.
7. Yudintsev, S.V., Stefanovsky, S.V., Kalenova, M.Yu., et al., *Radiochemistry*, 2015, vol. 57, no. 3, pp. 321–333.
8. Shoup, S.S., Bamberger, C.E., Haverlock, T.J., and Peterson, J.R., *J. Nucl. Mater*., 1997, vol. 340, pp. 112–117.
9. Yudintsev, S.V., Aleksandrova, E.V., Livshits, T.S., et al., *Dokl. Earth Sci.*, 2014, vol. 458, part 2, pp. 1281–1284.
10. Ewing, R.C., Weber, W.J., and Lutze, W., *Disposal of Weapon Plutonium*, Merz, E.R. and Walter, C.E., Eds., Amsterdam: Kluwer, 1996, pp. 65–83.
11. Weber, W.J., Ewing, R.C., Catlow, C.R.A., et al., *J. Mater. Res.,* 1998, vol. 13, no. 6, pp. 1434–1484.
12. Laverov, N.P., Yudintsev, S.V., Yudintseva, T.S., et al., *Geol. Ore Depos.*, 2003, vol. 45, no. 6, pp. 423–451.
13. Lumpkin, G.R., *Elements,* 2006. vol. 2, no. 6, pp. 365–372.
14. Allen, C.W. and Ryan, E.A., *Microsc. Res. Tech.*, 1998, vol. 24, pp. 255–259.
15. Lian, J., Wang, L.M., Sun, K., and Ewing, R.C., *Microsc. Res. Tech.,* 2009, vol. 72, pp. 165–181.
16. Lian, J., Wang, L.M., Ewing, R.C., and Boatner, L.A., *Nucl. Instr. Meth. Phys. Res. B*, 2005, vol. 241, pp. 365–371.
17. Park, S., Lang, M., Tracy, C.L., et al., *Acta Mater*., 2015, vol. 93, pp. 1–11.
18. Lang, M., Tracy, C.L., Palomares, R.I., et al., *J. Mater. Res*., 2015, vol. 30, no. 9, pp. 1366–1379.
19. Tracy, C.L., Shamblin, J., Park, S., et al., *Phys. Rev. B,* 2016, vol. 94, paper 064 102.
20. Lian, J., Chen, J., Wang, L.M., et al., *Phys. Rev. B,* 2003, vol. 68, paper 134 107.
21. Ewing, R.C., Weber, W.J., and Lian, J., *J. Appl. Phys.,* 2004, vol. 95, pp. 5949–5971.
22. Smith, K.L., Blackford, M.G., Lumpkin, G.R., et al., *Microsc. Microanal*., 2006, vol. 12, suppl. 2, pp. 1194–1196.
23. Whittle, K.R., Lumpkin, G.R., Blackford, M.G., et al., *J. Solid State Chem.,* 2010, vol. 183, pp. 2416–2420.
24. Havelia, S., Wang, S., Balasubramaniam, K.R., and Salvador, P.A., *J. Solid State Chem.*, 2009, vol. 182, pp. 1603–1610.

25. Morris, R.E., Owen, J.J., and Cheetham, A.K., *J. Phys. Chem. Solids*, 1995, vol. 56, pp. 1297–1303.
26. PDF-2 Database, Newtown Square (USA): Int. Centre for Diffraction Data, ICDD, 1998.
27. Weber, W.J., Nucl. *Instr. Meth. Phys. Res. B*, 2000, vols. 166–167, pp. 98–106.
28. Yudintsev, S.V., Stefanovsky, S.V., Nikol'skii, M.S., et al., *Radiochemistry*, 2016, vol. 58, no. 4, pp. 333–348.
29. Wang, S.X., Lumpkin, G.R., Wang, L.M., and Ewing, R.C., *Nucl. Instr. Meth. Phys. Res.* B, 2000, vols. 166–167, pp. 293–298.
30. Ziegler, J.F., Ziegler, M.D., and Biersack, J.P., *Nucl. Instr. Meth. Phys. Res. B*, 2010, vol. 268, pp. 1818–1823.
31. Yudintsev, S.V., Stefanovsky, S.V., and Ewing, R.C., *Structural Chemistry of Inorganic Actinide Compounds*, Krivovichev, S.V., Burns, P.C., and Tananaev, I.G., Eds., Amsterdam: Elsevier, 2007, pp. 457–490.
32. Laverov, N.P., Yudintsev, S.V., Livshits, T.S., et al., *Geochem. Int.*, 2010, vol. 48, no. 1, pp. 3–16.
33. Laverov, N.P., Yudintsev, S.V., Stefanovskii, S.V., et al., *Radiochemistry*, 2011, vol. 53, no. 3, pp. 229–243.
34. Yudintsev, S.V., Mal'kovskii, V.I., and Livshits, T.S., in *Materialy 15-i Mezhdunarodnoi konferentsii "Fiziko-khimicheskie i petrofizicheskie issledovaniya v naukakh o Zemle"* (Proc. 15th Int. Conf. "Physicochemical and Petrophysical Studies in Earth Sciences"), Moscow: Nauka, 2014, pp. 250–252.

Translated by G. Sidorenko